Final Draft
of the original manuscript:

Groll, N.; Widmann, M.:
Sensitivity of temperature teleconnections to orbital changes in AO-GCM simulations
In: Geophysical Research Letters (2006) AGU

DOI: 10.1029/2005GL025578

Sensitivity of temperature teleconnections to orbital changes in AO-GCM simulations

Nikolaus Groll

Institute for Coastal Research, GKSS Research Centre, Geesthacht, Germany

Martin Widmann

Institute for Coastal Research, GKSS Research Centre, Geesthacht, Germany

Teleconnections of interannual January air temperature variations over four regions are investigated based on quasi-equilibrium simulations with the general circulation model ECHO-G for three periods: the last interglacial (125 kyr BP - early Eemian); the last glacial inception (115 kyr BP) and the preindustrial period. The simulated teleconnections represent the teleconnection component due to internal climate variability and are in many regions closely linked to the temperature signal of the Arctic Oscillation.

The hemispheric-scale structure of temperature teleconnections is robust with respect to orbital forcing, but differences between the simulations are found on spatial scales up to several 1000 km. In the Eemian simulation teleconnections between temperatures in central Siberia (south of Greenland) and temperatures in many extratropical northern hemispheric regions are stronger (weaker) compared to the other two simulations, while teleconnections for northeastern and western Europe show more complex differences.

1. Introduction

Variations in incoming solar radiation due to changes in solar output and in the earth's orbit can affect atmospheric temperature and circulation. Regional temperatures can be directly influenced by variations in the incoming solar radiation in a given area, but also by circulation changes. A response of atmospheric circulation to insolation forcing has been found in many simulations with general circulation models (GCMs) [e.g. *Cubasch et al.*, 1997; *Kaspar et al.*, 2005; *Hall et al.*, 2005]. During the early Eemian a positive Arctic Oscillation index (AOI) relative to the preindustrial period has been noted [*Felis et al.*, 2004]. This change of the AOI is consistent with the mean simulated SLP difference between the Eemian and the preindustrial period presented in *Groll et al.* [2005]. The latter study showed that the differences in the mean and variability of circulation lead to changed relationships between multi-decadal variations in the AOI and regional temperature.

A physical explanation for the AO response to changes in the meridional temperature gradient was given by *Robinson* [2000] and by *Kushnir et al.* [2002], who point out that the associated changes in the generation of lower-tropospheric baroclinic eddies and in the upper-tropospheric convergence of the eddy momentum flux lead to an AO-like change of the Northern Hemispheric circulation. *Hall et al.* [2005] demonstrated the relevance of this mechanism for orbitally controlled circulation changes over the last 165000 years.

0094-8276/06/$5.00

Here we focus on the sensitivity of interannual temperature teleconnections to changes in the orbital forcing and analyze coupled atmosphere-ocean GCM simulations for the preindustrial period, the last interglacial and the last glacial inception. In order to understand this sensitivity, we investigate the link between temperature teleconnections and circulation. Note that we use the term teleconnections for the hemispheric pattern of correlation coefficients between temperatures in a given area and those at all other locations, excluding the positive correlations in the vicinity of the center region.

An improved understanding of teleconnections helps to decide whether temperature-sensitive proxy records from different regions can be expected to have similar or opposite variations. Networks of temperature-sensitive proxy records with high enough temporal resolution and absolute dating accuracy to investigate teleconnections are not available for the periods investigated in this paper. Therefore we use model simulations as a surrogate for the real climate to investigate teleconnections of high-frequency temperature variability.

Our study uses quasi-equilibrium simulations and thus temperature variations within a simulation are entirely due to internal variability (mainly atmospheric circulation variability). In the real world changing forcing factors such as solar variability or volcanic aerosols also affect temperatures on interannual to decadal time scales. To the extent that the simulated circulation variability is realistic, the simulated temperature teleconnections account for the component in the real-world teleconnections that is due to internally generated variability, and also for the component that is due to forced circulation variability with the same structure as the internally generated variability. This study should therefore be viewed as a first step towards a systematic understanding of the teleconnections of regional temperatures and of their sensitivity to the structure of the large-scale circulation, which in turn is related to orbital forcing.

We focus on January, because in winter high-frequency temperature variations are mostly dominated by large-scale circulation variability and thus a noticeable link between circulation changes and temperature teleconnections can be expected. Similar results for other boreal winter months and for decadal variability have been obtained, but are not shown.

2. Model description and experimental setups

This study is based on simulations with the coupled atmosphere-ocean GCM ECHO-G. It consists of the atmospheric model ECHAM-4 [*Roeckner et al.*, 1996] and the ocean model HOPE [*Wolff et al.*, 1997], in a version that includes a thermodynamic-dynamic sea-ice model (HOPE-G). The atmospheric model uses a spectral resolution of T30

(approx. 3.75° x 3.75°) with 19 vertical levels. The ocean model has a horizontal resolution of about 2.8° x 2.8° with a grid refinement in the tropical regions and 20 vertical levels. To avoid a climate drift in long simulations a constant-in-time flux adjustment is applied.

Three existing quasi-equilibrium simulations are analyzed: one for present day insolation with preindustrial (A.D. 1800) greenhouse gas concentrations (hereafter PI) [*Lorenz and Lohmann*, 2004]; one for the Eemian - the last interglacial - at 125 kyr BP (hereafter EEM) [*Kaspar et al.*, 2005] and one for the last glacial inception (hereafter GI) at 115 kyr BP [*Cubasch et al.*, 2005]. Insolation for a given set of orbital parameters is calculated according to *Berger* [1978], greenhouse gas concentrations (GHG conc.) are taken from the Vostok ice core [*Petit et al.*, 1999; *Sowers*, 2001], and vegetation is fixed to its modern state in all simulations. After a model spin up of 1300 (1000) years for PI (EEM and GI), a 1000 yr long simulation period is analyzed. Orbital parameters and GHG conc. of the three simulations are shown in Table 1. In January the insolation gradient between the North Pole and the Equator is lower by about $40 Wm^{-2}$ in EEM and $20 Wm^{-2}$ higher in GI compared to PI. GHG conc. differences between the three simulations are small and it can be expected that the differences in the simulated climate are mainly due to the changed orbital parameters.

3. Teleconnections of regional temperatures

We analyze teleconnections of the interannual variability of January temperatures in the three GCM simulations for four regions: the region south of Greenland (SG); western Europe (WE); northeastern Europe (NE) and central Siberia (CS). In these regions temperature variability is dominated by atmospheric circulation variability, particularly during winter. Regional temperature series are defined as the spatial mean of six grid cells from the 2m temperature field. We use 1000 years from each simulation to calculate the correlation between detrended simulated monthly temperature means from the specified regions and detrended monthly temperatures at all other grid cells in the extratropical Northern Hemisphere. All discussed differences between the three simulations are significant at the 5% level and are robust when different 500year long subperiods are considered.

As expected each region shows in all simulations an area with high positive correlation coefficients around its center (Fig.1). Although the large-scale spatial structure of the teleconnections is similar in all simulations, there are small, but clearly noticeable differences between EEM and PI for some regions (Fig.1, bottom panels). SG temperatures show weaker teleconnections over large parts of the North/East Atlantic and Arctic Ocean and along the east coast of North America in EEM compared to PI. Teleconnections of WE temperatures are weaker or change sign over the Labrador Sea and south of Greenland in EEM compared to PI. Teleconnection changes for NE temperatures are evident in the Gulf of Mexico, east of Greenland and parts of Siberia. CS temperature teleconnections are stronger west of Greenland and over northwest Russia and the Mediterranean in EEM than in PI. The teleconnection differences between GI and PI are small and therefore not shown.

4. Relation to changes in the AO-temperature signal

Teleconnections between interannual winter temperatures can be expected to be mainly caused by large-scale circulation variability. We thus investigate how the changes in the temperature teleconnections are related to changes in the AO-temperature signal. *Groll et al.* [2005] showed that the AO-temperature signal is sensitive to changes in the orbital forcing on multi-decadal time scales. They suggested that these differences in the AO-temperature signal result from a more zonal mean flow in the early Eemian compared to the preindustrial period, which leads to a shift of the maximum of the AO-temperature signal from Europe to Siberia. We express the AO-temperature signal as the correlation coefficients between the AOI and the 2m January temperatures and, in contrast to *Groll et al.* [2005], consider annual resolution. The AOI is defined as the first principal component of extratropical (20°-90°N) sea level pressure.

All three simulations yield a similar spatial distribution of correlation coefficients (Fig.2). However, there are small differences in the position of the nodes and centers of the AO-temperature signal. For instance correlations are weaker over Northwest Europe and the Labrador Sea and higher over Siberia in EEM compared to the other simulations. These differences correspond to the weaker teleconnections for SG and WE in EEM shown in Fig.1, which indicates that these temperature teleconnections are related to the AO-temperature signal and thus a weaker link between the AOI and regional temperatures leads to weaker temperature teleconnections. The higher AO-temperature correlations over Siberia and the stronger CS teleconnection with northwest Russia and the Mediterranean (Fig.1) also confirm this relationship.

The hypothesis that temperature teleconnections are closely related to the AO-temperature signal is corroborated by pattern correlation maps, in which the value at each grid cell is given by the latitude-weighted pattern correlation between the AO-temperature signal and the temperature teleconnection map for this grid cell. These pattern correlations maps (Fig.3) resemble the AO-temperature signal (Fig.2). Hence temperature teleconnections are similar to the AO-temperature signal for all regions where the AO-temperature signal is moderate to strong.

Differences of the pattern correlation maps from the different simulations show large areas with smaller correlations in EEM compared to PI, but also higher correlations over Siberia, which is consistent with the weaker AO-temperature signal over SG and WE, a stronger signal over CS, and a similar signal over NE. Differences between GI and PI are only small and therefore not shown.

5. Conclusions

Our results, which are based on quasi-equilibrium GCM simulations, suggest that the component of real-world temperature teleconnections that is due to internally generated variability is moderately sensitive to orbital forcing, i.e. the hemispheric-scale structures of teleconnections are similar, but clearly noticeable differences exist over regions up to several 1000 km. Pattern correlations between the AO-temperature signal and temperature teleconnections indicate that the AO is in many regions the main reason for temperature teleconnections.

Differences in teleconnections are found between the early Eemian and the preindustrial simulation, but not between the glacial inception and the preindustrial simulation. These differences in temperature teleconnection may be relevant for understanding links between temperature-sensitive proxy data with high temporal resolution from different regions.

Acknowledgments. We thank Julie M. Jones, Kerstin Prömmel and two anonymous reviewers for their valuable comments which helped to improve the manuscript. We also thank Frank Kaspar and Stephan J. Lorenz for providing their model simulations. Beate Gardeike is acknowledged for help with figure preparation. This work was funded within the EEM project (Climate change at the very end of a warm stage) by the Federal Ministry of Education and Research under the DEKLIM program (Deutsches Klimaforschungsprogramm).

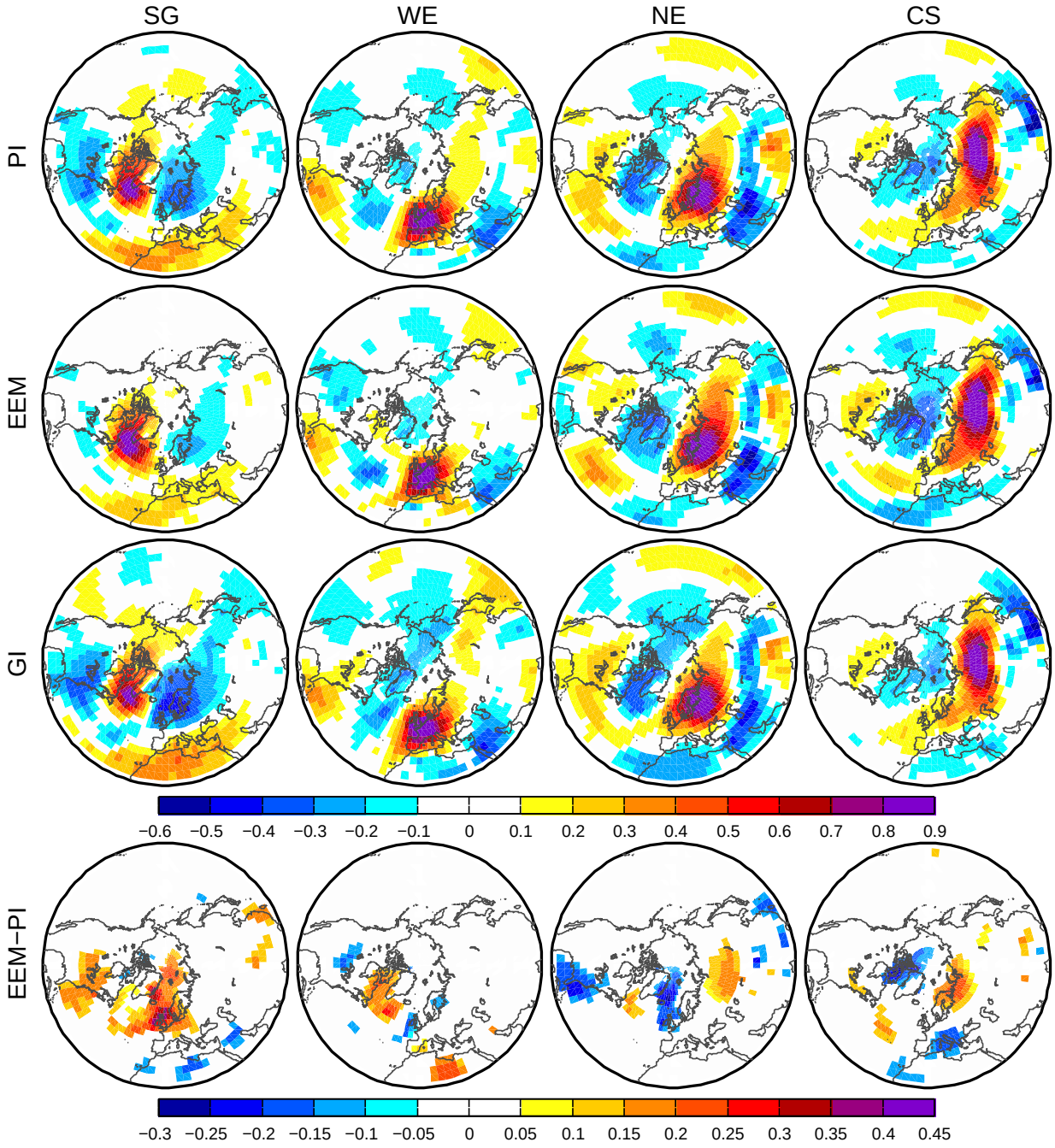

Figure 1. Teleconnections in (top) PI, (second row) EEM, (third row) GI, and (bottom) differences EEM-PI for annually resolved 2m January temperatures. Shown are correlation coefficients between detrended extratropical Northern Hemisphere grid cell temperatures and four regional temperatures derived as the spatial mean of six grid cells that represents: south of Greenland (SG); western Europe (WE); northeastern Europe (NE); central Siberia (CS). All correlations and differences shown are significant at the 5% level.

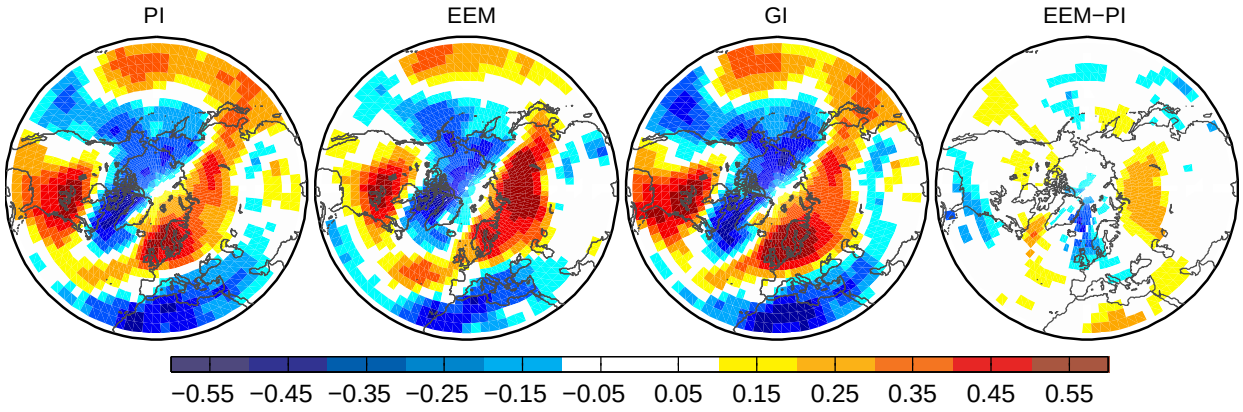

Figure 2. January AO-temperature signal as correlation coefficients between the AOI and 2m temperature for (left) PI, (second) EEM, (third) GI and (right) difference EEM-PI. All correlations and differences shown are significant at the 5% level.

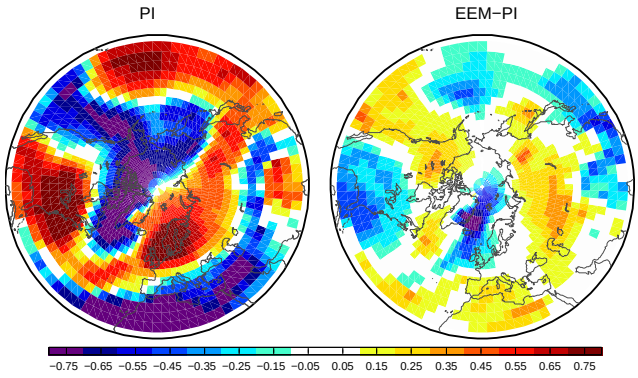

Figure 3. Pattern correlation between one-point temperature correlation maps and the AO-temperature signal for (left) PI and (right) difference EEM-PI. All correlations and differences shown are significant at the 5% level.

Table 1. Greenhouse gas concentration (GHG conc.) and earth orbital parameters used in the three experiments (exp). PI: simulation with preindustrial GHG conc. and today's orbital parameters; EEM and GI: simulation with GHG conc. and orbital parameters of 125 kyr BP and 115 kyr BP respectively.

exp	CO_2 (ppm)	CH_4 (ppb)	N_2O (ppb)	Eccent. (%)	Obliquity axis tilt (°)	Perihelion (°)
PI	280	700	310	1.67	23.44	282.7
EEM	270	630	260	4.00	23.79	127.3
GI	265	520	270	4.14	22.41	290.9

References

Berger, A. L., Long-term variations of daily insolation and Quaternary climatic changes, *J. Atmos. Sci.*, *35*, 2362–2367, 1978.

Cubasch, U., G. C. Hegerl, R. Voss, J. Waszkewitz, and T. C. Crowley, Simulation with an O-AGCM of the influence of variations of the solar constant on the global climate, *Clim. Dynam.*, *13*, 757–767, 1997.

Cubasch, U., E. Zorita, F. Kaspar, K. Prömmel, H. von Stroch and F. Gonzales-Rouco, Simulation of the role of solar forcing on climate, *Advances in Space Research*, in press, doi: 10.1016/j.asr.2005.04.07, 2005.

Felis, T., G. Lohmann, H. Kuhnert, S. J. Lorenz, D. Scholz, J. Pätzold, S. A. Al-Rousan, and S. M. Al-Moghrabi, Increased seasonality in Middle East temperatures during the last interglacial period, *Nature*, *429*, 164–168, 2004.

Groll, N., M. Widmann, J. M. Jones, F. Kaspar, and S. J. Lorenz, Simulated Relationships between Regional Temperatures and Large-Scale Circulation: 125 kyr BP (Eemain) and the Preindustrial Period, *J. Climate*, *18*(19), 4035–4048, doi: 10.1175/JCLI3469.1, 2005.

Hall, A., A. Clement, D. W. J. Thompson, A. Broccoli, and C. Jackson, The Importance of Atmospheric Dynamics in the Northern Hemisphere Wintertime Climate Response to Changes in the Earth's Orbit, *J. Climate*, *18*(9), 1315–1325, doi:10.1175/JCLI3327.1, 2005.

Kaspar, F., N. Kühl, U. Cubasch, and T. Litt, A model-data-comparison of European temperatures in the Eemian interglacial, *Geophys. Res. Lett.*, *32*(11), L11703, doi: 10.1029/2005GL02245, 2005.

Kushnir, Y., W. A. Robinson, I. Blade, N. M. J. Hall, S. Peng, and R. Sutton, Atmospheric GCM response to extratropical SST anomalies: Synthesis and evaluation, *J. Climate*, *15*, 2233–2256, 2002.

Lorenz, S. J., and G. Lohmann, Acceleration technique for Milankovitch type forcing in a coupled atmosphere-ocean circulation model: method and application for the Holocene, *Clim. Dynam.*, *23*, 727–743, doi:10.1007/s00382-004-0469-y, 2004.

Petit, J. R., et al., Climate and atmospheric history of the past 420,000 years from the Vostok ice core - antarctica, *Nature*, *399*, 429–436, 1999.

Robinson, W. A., A baroclinic mechanism for the eddy feedback on the zonal index, *J. Atmos. Sci.*, *57*, 415–422, 2000.

Roeckner, E., et al., The atmosphere general circulation model ECHAM-4: model description and simulation of present-day climate, *Technical Report 218*, Max-Planck Institute for Meteorology, 1996.

Shindell, D. T., G. A. Schmidt, M. E. Mann, D. Rind, and A. Waple, Solar Forcing of Regional Climate Cange During the Maunder Minimum, *Science*, *294*, 2149–2152, 2001.

Sowers, T., N_2O record spanning the penultimate deglaciation from the Vostok ice core, *J. Geophys. Res.*, *106*(D23), 31,903–31,914, 2001.

Wolff, J. O., E. Maier-Reimer, and S. Legutke, The Hamburg Ocean Primitive Equation Model HOPE, *Technical Report 13*, German Climate Computing Center (DKRZ), 1997.

Zorita, E., H. von Storch, F. J. Gonzales-Rouco, U. Cubasch, J. Luterbacher, S. Legutke, I. Fischer-Bruns, and U. Schlese, Climate Evolution in the Last Five Centuries Simulated by an Atmosphere- Ocean Model: Global Temperatures, the North Atlantic Oscillation and the Late Maunder Minimum, *Meteor. Z.*, *13*(4), 271–289, 2004.

Nikolaus Groll, Institute for Coastal Research, GKSS Research Centre, D21502 Geesthacht, Germany. (groll@gkss.de)